



Theoretical Study on the Effect of Triphenylamine on the Electronic, Optical and Charge Transport Properties of 2,1,3-Benzothiadiazole-Based Derivative

B. HU^{1,2,*}, C. YAO^{1,2} and R.F. JIN³

¹Faculty of Chemistry, Jilin Normal University, Siping 136000, P.R. China

²Key Laboratory of Preparation and Applications of Environmental Friendly Materials, Ministry of Education, Jilin Normal University, P.R. China

³College of Chemistry and Chemical Engineering, Chifeng University, Chifeng 024000, P.R. China

*Corresponding author: Fax: +86 434 3291861; Tel: +86 434 3295669; E-mail: hubo97@yahoo.cn

(Received: 18 March 2011;

Accepted: 5 December 2011)

AJC-10796

A investigation of the variation in electronic, optical and charge transport properties upon the change of the molecular structure in 2,1,3-benzothiadiazole (BTD)-based derivative is presented using quantum-chemical approaches. Our quantum chemical calculations reveal that removing one triphenylamine unit in the backbone causes blue-shift in both the absorption and emission spectra relative to the pristine molecule. Such blue-shifts are attributed to the increase of the energy gap for the frontier molecular orbitals involved in the absorption and emission transitions. In addition, from the reorganization energy values based on charge hopping model, it is found that hole transportation is remarkably improved when removing one triphenylamine unit in the backbone, suggesting studied 2,1,3-benzothiadiazole-based derivative to be good hole transport material in organic light-emitting diodes.

Key Words: Triphenylamine, 2,1,3-Benzothiadiazole, Electronic and optical properties, Reorganization energy.

INTRODUCTION

Donor(D)-acceptor(A) molecules featuring benzothiadiazole and amino groups have been shown as attractive candidates for electro-optic applications, because their architecture, including the low-bandgap core and suitably substituted peripheral functional groups, leads to molecules with tunable emission characteristics, enhanced hole/electron affinity and promising thermal characteristics¹. Furthermore, a series of donor- π -bridge-acceptor- π -bridge-donor (D- π -A- π -D)-type benzothiadiazole-based dyes possessing terminal *N,N*-disubstituted amino groups have been provided with high fluorescence quantum yields among the orange-red colour region as well as large two-photon absorption cross-sections in the near IR region². Among these materials, 4,7-bis[4-(*N,N*-diphenylamino)phenyl]-2,1,3-benzothiadiazole (OMC, Fig. 1), bearing 2,1,3-benzothiadiazole (BTD), two diphenylamine and two benzene spacers, belongs to D- π -A- π -D-type molecule and shows great potential application in organic light-emitting diodes (OLEDs). So far, considerable effort has been focused on understanding the electronic structure and optical properties of various light-emitting materials. Therefore, in this paper, we provide a theoretical investigation on the variation in electronic, optical and charge transport properties upon the change of the molecular structure along the backbone in OMC, aim at understanding of the structure-property relationships and thus

acquiring important insights into the design of new light-emitting materials.

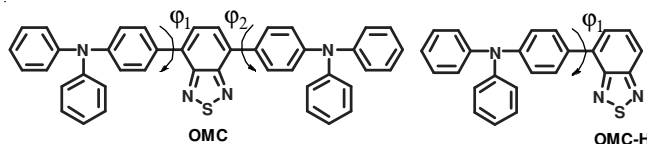


Fig. 1. Chemical structures of the investigated BTD-based derivatives OMC and OMC-H

COMPUTATIONAL DETAILS

The considered molecular structures are plotted in Fig. 1. Structurally, OMC is composed of three parts: triphenylamine (TPA), BTD and TPA, while OMC-H is composed of two parts: TPA and BTD. All the quantum-chemical calculations were performed with the Gaussian 03 software package³. In this respect, it is worthwhile to mention that the details about the method determination of the geometry optimizations and the absorption and emission spectra can be found in previous work⁴. The ground-state (S_0) geometry optimizations were carried out at the *ab initio* Hartree-Fock (HF)⁵ level of theory. Electronic properties in S_0 were calculated using density functional theory (DFT)⁶ with the PBE0⁷ hybrid functional. By employing the *ab initio* configuration interaction singles (CIS)⁸ approach, the excited-state (S_1) geometries were

optimized. The absorption and emission spectra were computed at the optimized S_0 and S_1 geometries with time-dependent DFT (TD-DFT)⁹ using PBE0 functional, respectively. The 6-31G(d)¹⁰ split valence polarized basis set was employed through out. The reorganization energy were also estimated from the single point energy at the B3LYP/6-31G(d,p)¹⁰ level based on the PBE0/6-31G(d) optimized neutral, cationic and anionic geometries.

RESULTS AND DISCUSSION

A schematic representation for the energy levels of the highest occupied molecular orbital (HOMO) and the lowest unoccupied molecular orbital (LUMO) in S_0 of the OMC and OMC-H is depicted in Fig. 2a. Fig. 2a clearly presents that both the energies of the HOMO (E_{HOMO}) and the LUMO (E_{LUMO}) of OMC-H decrease in comparison with those of OMC. The E_{HOMO} decreases more than E_{LUMO} in OMC-H, thus the energy gaps (E_g) increases with respect to that of OMC.

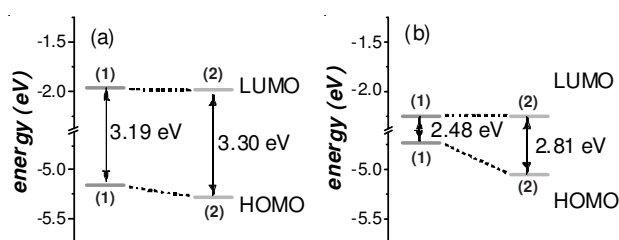


Fig. 2 (a) Scheme of frontier molecular orbital levels calculated at the PBE0/6-31G(d)//HF/6-31G(d) level of theory; (b) Scheme of frontier molecular orbital levels calculated at the TD-PBE0/6-31G(d)//CIS/6-31G(d) level of theory. (1): OMC; (2): OMC-H

In order to understand the electron transport in molecular devices, we analyze the shape of the frontier molecular orbitals (FMOs). Fig. 3a displays the electronic density distribution of the HOMOs and LUMOs for OMC and OMC-H. As shown in Fig. 3a, the LUMO and HOMO of OMC-H have essentially the same electron density distribution as those of OMC and the LUMO is mostly centralized on BTM and the HOMO is mainly localized on TPA.

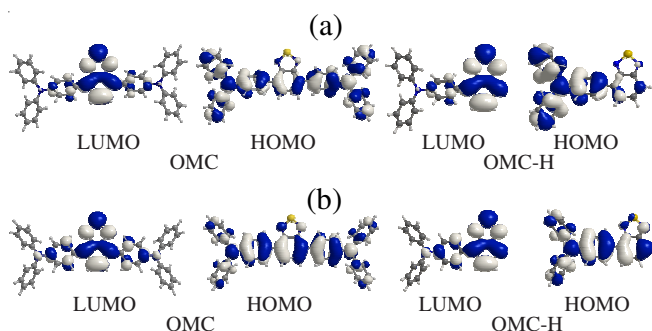


Fig. 3. (a) HOMOs and LUMOs of OMC and OMC-H calculated at the PBE0/6-31G(d)//HF/6-31G(d) level of theory; (b) HOMOs and LUMOs of OMC and OMC-H calculated at the TD-PBE0/6-31G(d)//CIS/6-31G(d) level of theory

The vertical excitation energies (E_v), the maximum absorption/emission wavelength ($\lambda_{\text{abs}}/\lambda_{\text{em}}$) and corresponding oscillator strength (f) for OMC and OMC-H are collected in

Table-1. λ_{abs} and λ_{em} values of OMC-H are blue-shifted by 23.1 and 90 nm compared to OMC (Fig. 4). The change for $\lambda_{\text{abs}}/\lambda_{\text{em}}$ can be ascribed to the variation of E_g (Fig. 2). Moreover, Table-1 and Fig. 4 clearly indicate that the oscillator strength for the absorption and emission spectra of OMC-H are too small with respect to OMC. The electron transition at the λ_{abs} corresponds to the promotion of an electron from HOMO to LUMO exclusively. While the emission reversely corresponds to an electron transition configuration: LUMO \rightarrow HOMO. As shown in Fig. 3, the LUMOs in the S_0 and S_1 show the same qualitative picture, this is mostly localized on BTM. The HOMOs comparing the S_0 and S_1 are much different. In OMC and OMC-H, the contribution from the phenyl ring of BTM, the spacer phenyl ring of TPA increase, while that from another two phenyl rings of TPA decrease. Inspection of the optimized S_1 and S_0 geometries of OMC and OMC-H reveals that, great geometric changes from S_0 to S_1 take place at the dihedral angles φ_1 and φ_2 (Fig. 1). For OMC, the φ_1 and φ_2 values of 18.88° and 18.87° in S_1 are much smaller than the corresponding values of 45.17° and 45.17° in S_0 . For OMC-H, the φ_1 of 13.35° in S_1 are significantly decreased with respect to the corresponding value of ca. 45.17° in S_0 . This suggests that S_1 geometries are more coplanar compared to those in S_0 and reducing φ_1 and φ_2 enhance the degree of π -conjugation between TPA and BTM. Thus, the HOMOs of OMC and OMC-H are mainly localized on the phenyl ring of BTM, the spacer phenyl ring of TPA. By reference to Fig. 3, both the absorption/emission process can be described as a charge transfer transition from TPA (donor) to BTM (acceptor)/from BTM to TPA.

TABLE-1
OPTICAL PROPERTIES OF OMC AND OMC-H COMPUTED AT THE TD-PBE0/6-31G(d) LEVEL

| | Absorption properties | | | Emission properties | | |
|-------|-----------------------|------------------------|------|---------------------|-----------------------|------|
| | E_v | λ_{abs} | f | E_v | λ_{em} | f |
| OMC | 2.63 | 471.2 | 0.44 | 2.01 | 617.1 | 0.79 |
| OMC-H | 2.77 | 448.1 | 0.16 | 2.35 | 527.1 | 0.38 |

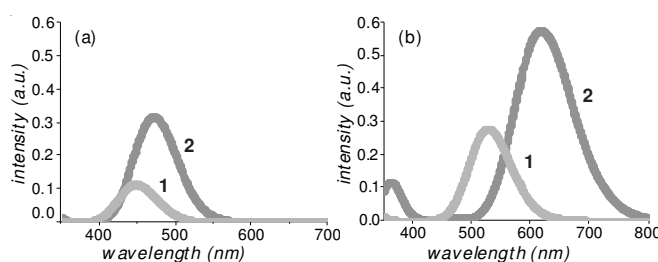


Fig. 4. (a) Absorption spectra of OMC and OMC-H; (b) Emission spectra of OMC and OMC-H; (1): OMC; (2): OMC-H

It is known that the charge-carrier (hole and electron) transport property is a key factor in the performance of organic light-emitting diodes. We mainly investigated the effect of the internal reorganization energy (λ_h/λ_e for hole/electron) in the charge transfer process. Our calculations of the reorganization energy associated with different geometries of two states are based on the hopping model. The results summarized in Table-2 show that, λ_h is smaller than that of N,N'-diphenyl-N,N'-bis(3-methylphenyl)-(1,1'-biphenyl)-4,4'-diamine (TPD), which is a typical hole transport material ($\lambda_h = 0.290$ eV)¹¹. The smaller

λ value is, the bigger the charge-carrier transport rate is. λ_h value is smaller than its respective λ_e , indicating that the carrier mobility of the hole is larger than that of the electron for OMC-H. It implies that OMC-H can be used as better hole transport material in the organic light-emitting diodes. Noticeably, λ_h and λ_e values of OMC-H decrease in comparison with those of OMC, indicating the improved hole and electron transportations upon the removing of one TPA unit in the backbone of OMC.

TABLE-2
INTRAMOLECULAR REORGANIZATION
ENERGIES (eV) OF OMC AND OMC-H

| | Reorganization for hole | | | Reorganization for electron | | |
|-------|-------------------------|----------------|---|-----------------------------|----------------|---|
| | λ_{h1} | λ_{h2} | $\lambda_h = \lambda_{h1} + \lambda_{h2}$ | λ_{e1} | λ_{e2} | $\lambda_e = \lambda_{e1} + \lambda_{e2}$ |
| OMC | 0.143 | 0.087 | 0.230 | 0.176 | 0.322 | 0.498 |
| OMC-H | 0.088 | 0.049 | 0.137 | 0.178 | 0.275 | 0.453 |

Conclusion

Theoretical investigations on the variation in electronic, optical and charge transport properties upon the change of the molecular structure in OMC have been performed. The removing of one TPA unit in the backbone of OMC decreases both the E_{HOMO} and E_{LUMO} relative to OMC. Thus, the increased E_g value is obtained in OMC-H with respect to that of OMC. OMC-H has essentially the same electron density distribution of the LUMO and HOMO as those of OMC. OMC-H presents shorter $\lambda_{\text{abs}}/\lambda_{\text{em}}$ than OMC, which is ascribed to the variation of E_g . Low λ_h is also obtained based on OMC-H, indicating that OMC-H can be used as better hole transport material in the organic light-emitting diodes. This work may provide a useful insight for designing high-performance functional materials.

ACKNOWLEDGEMENTS

Financial supports from the Education Office of Jilin Province (No. 2010142) and Institute Foundation of Siping City (No.

2010009) are gratefully acknowledged. The authors also thank State Key Laboratory of Theoretical and Computational Chemistry of Jilin University for providing program supports.

REFERENCES

1. K.R. Justin Thomas, J.T. Lin, M. Velusamy, Y.T. Tao and C.H. Chuen, *Adv. Funct. Mater.*, **14**, 83 (2004).
2. S.I. Kato, T. Matsumoto, M. Shigeiwa, H. Gorohmaru, S. Maeda, T. Ishi-I and S. Mataka, *Chem. Eur. J.*, **12**, 2303 (2006).
3. M.J. Frisch, G.W. Trucks, H.B. Schlegel, G.E. Scuseria, M.A. Robb, J.R. Cheeseman, J.A. Montgomery, Jr., T. Vreven, K.N. Kudin, J.C. Burant, J.M. Millam, S.S. Iyengar, J. Tomasi, V. Barone, B. Mennucci, M. Cossi, G. Scalmani, N. Rega, G.A. Petersson, H. Nakatsuji, M. Hada, M. Ehara, K. Toyota, R. Fukuda, J. Hasegawa, M. Ishida, T. Nakajima, Y. Honda, O. Kitao, H. Nakai, M. Klene, X. Li, J.E. Knox, H.P. Hratchian, J.B. Cross, C. Adamo, J. Jaramillo, R. Gomperts, R.E. Stratmann, O. Yazyev, A.J. Austin, R. Cammi, C. Pomelli, J.W. Ochterski, P.Y. Ayala, K. Morokuma, G.A. Voth, P. Salvador, J.J. Dannenberg, V.G. Zakrzewski, A.D. Daniels, O. Farkas, A.D. Rabuck, K. Raghavachari and J.V. Ortiz, Gaussian 03, Revision B.03; Gaussian, Inc., Pittsburgh, PA (2003).
4. (a) B. Hu and J.P. Zhang, *Polymer*, **50**, 6172 (2009); (b) B. Hu, J.P. Zhang and Y. Chen, *Eur. Polym. J.*, **47**, 208 (2011).
5. (a) C.C.J. Roothaan, *Rev. Mod. Phys.*, **23**, 69 (1951); (b) J.A. Pople and R.K. Nesbet, *J. Chem. Phys.*, **22**, 571 (1954); (c) R. McWeeny and G. Diercksen, *J. Chem. Phys.*, **49**, 4852 (1968).
6. R.G. Parr and W. Yang, *Density Functional Theory of Atoms and Molecules*. Oxford University Press: Oxford (1989).
7. (a) M. Ernzerhof and G.E. Scuseria, *J. Chem. Phys.*, **110**, 5029 (1999). (b) C. Adamo and V. Barone, *J. Chem. Phys.*, **110**, 6158 (1999).
8. J.B. Foresman, M. Head-Gordon, J.A. Pople and M.J. Frisch, *J. Phys. Chem.*, **96**, 135 (1992).
9. (a) R.E. Stratmann, G.E. Scuseria and M.J. Frisch, *J. Chem. Phys.*, **109**, 8218 (1998); (b) R. Bauernschmitt and R. Ahlrichs, *Chem. Phys. Lett.*, **256**, 454 (1996); (c) M.E. Casida, C. Jamorski, K.C. Casida and D.R. Salahub, *J. Chem. Phys.*, **108**, 4439 (1998).
10. (a) P.C. Hariharan and J.A. Pople, *Mol. Phys.*, **27**, 209 (1974); (b) M.S. Gordon, *Chem. Phys. Lett.*, **76**, 163 (1980); (c) M.J. Frisch, J.A. Pople and J.S. Binkley, *J. Chem. Phys.*, **80**, 3265 (1984).
11. M. Malagoli and J.L. Brédas, *Chem. Phys. Lett.*, **327**, 13 (2000).